PROCEEDINGS OF SCIENCE

Electron and Photon reconstruction and identification with the CMS detector in pp collisions at $\sqrt{s}$ = 7 TeV

Salerno Roberto*
LLR-Ecole Polytechnique
E-mail: roberto.salerno@cern.ch

The performance of electron and photon reconstruction and identification in CMS has been studied at $\sqrt{s}$ = 7 TeV. Reconstruction and identification variables as well as isolation variables have been compared between data and Monte Carlo for signal and background. Electron reconstruction and selection efficiencies, electron fake rate and photon purity have been determined and compared with Monte Carlo predictions. Level 1 Trigger and High Level Trigger efficiencies have been measured. In this work the data collected correspond to an integrated luminosity of $\mathscr{L}_{int}$ = 200 nb^{-1}.

35th International Conference of High Energy Physics
July 22-28, 2010
Paris, France

*Speaker.

PoS(ICHEP 2010)022

During the 2010 run, the Large Hadron Collider (LHC) [1] at CERN collided beams of protons at a centre of mass energy of $\sqrt{s}$ = 7 TeV In this work, data corresponding to 200 nb^{-1} were used to study electron and photon reconstruction and identification in the Compact Muon Solenoid (CMS) experiment. A detailed description of the CMS detector can be found elsewhere [2].

1. Electron/Photon triggers

The L1 e/γ trigger decision is based on electron/photon trigger candidates which uses local energy deposits called trigger primitives as inputs. Details on the ECAL trigger algorithm can be found in [2]. At HLT, electron and photon selection proceeds requiring a supercluster with ET above a given threshold matching an electromagnetic L1 candidate. The HLT runs the standard ECAL super- clustering algorithm with almost identical settings to the offline reconstruction. The electron paths additionally require a hit in the pixel layers of the CMS detector compatible with an electron trajectory, with matching requirements currently looser than the offline requirements in most regions of the detector. More details on the electron HLT can be found in [2].

Figure 1 shows the L1 SingleEG5 trigger efficiency with respect to reconstructed electrons and the HLT Photon15 trigger efficiency with respect to an offline electron which has already produced a L1 SingleEG5 candidate.

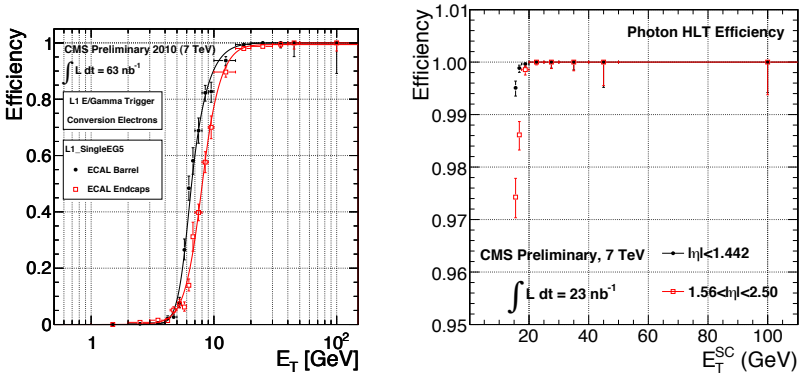

(a) (b)

Figure 1: L1 and HLT efficiency results: (a) L1 SingleEG5 trigger efficiency for electron candidates from minimum bias data (b) HLT Photon15 efficiency for an offline reconstructed electron matched to a L1 SingleEG5 candidate, as a function of the electron supercluster transverse energy for candidates in the ECAL barrel (black dots) and in the ECAL endcaps (red empty squares).

2. Electron reconstruction and identification

Electron reconstruction uses two complementary algorithms at the track seeding stage: a 'tracker driven' seeding, more suitable for low pT electrons as well as performing better for electrons inside jets and 'ECAL driven' seeding. The 'ECAL driven' algorithm starts by the reconstruction of ECAL "superclusters" of transverse energy ET > 4 GeV and is optimized for isolated electrons in the pT range relevant for Z or W decays and down to pT = 5 GeV/c. The reconstruction then proceeds with a dedicated track algorithm [3] and finally a preselection based on track-supercluster match. More details on electron reconstruction can be found here [4].

2.1 Measurement of the reconstruction and selection efficiencies

The baseline method for the measurement of the electron reconstruction efficiency relies on "tag-and-probe" from Z decays Ref. [6]. A well defined, identified and isolated electron is used as the "tag". Approximately 70 Z→ee events have been used to measure the reconstruction efficiency. An efficiency value of 99.3% ± 1.4% (resp. 96.8% ± 3.4%) is obtained for electrons in the ECAL barrel (resp. in the ECAL endcaps), in good agreement with the expected efficiency from the Monte Carlo simulation of 98.5% (resp. 96.1%).

The first approach to electron selection is to use simple cuts on the variables measuring spatial matching between the track and the supercluster ($\Delta\eta_{in}$ and $\Delta\phi_{in}$), the supercluster η width ($\sigma_{i\eta i\eta}$), and the hadronic leakage variable (H/E). Figure 2 presents the distributions for tagged signal electron candidates of some electron ID variables.

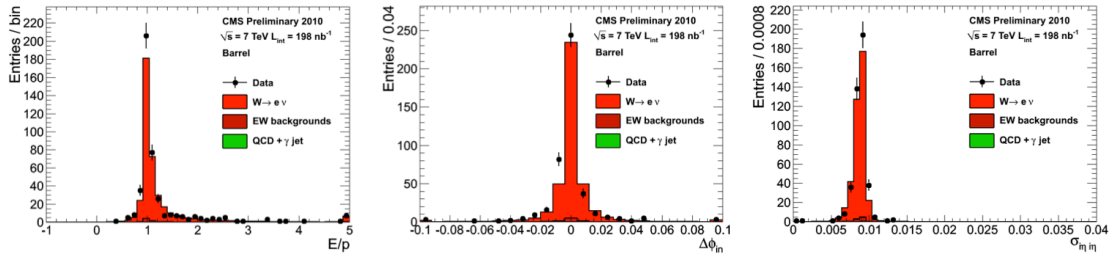

(a) (b) (c)

Figure 2: Distribution of electron ID variables for tagged electron candidates from W events in data (dots) compared with Monte Carlo (histograms): (a) the ratio E/p of the supercluster energy in the ECAL over the track momentum at the innermost state, (b) $\Delta\phi_{in}$ and (c) $\sigma_{i\eta i\eta}$. Distributions are for the ECAL barrel. The distributions are normalized to the integrated luminosity

Different cuts are used in the ECAL barrel and the ECAL endcaps. A series of reference selections have been produced using Monte Carlo samples, we consider here only two working points 95% (WP95) and the 80% (WP80). The effect of the application of the selection on signal and background can be seen in an inclusive sample of electron with ET > 25 GeV as shown in Figure 3.

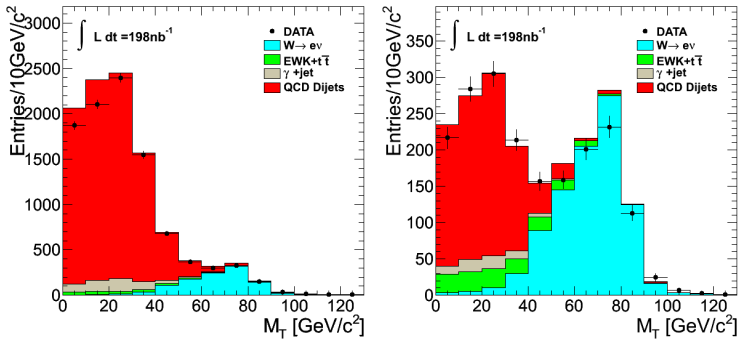

(a) (b)

Figure 3: Transverse mass distribution for candidates with supercluster ET >25 GeV in data (dots) compared with Monte Carlo (histograms) after (a) WP95 and (b) WP80 selections.

The second approach to electron selection is to separate electron candidates into categories according to observables that are sensitive to the amount of bremsstrahlung [4]. These variables are the fraction f_{brem} of radiated energy as measured from the innermost and outermost state of the electron track and the ratio E/p between the supercluster energy and the measured track momentum at the vertex. We consider here only two working points which we will refer as "CiC Loose" and "CiC SuperTight", respectively targeted for efficiency of about 95% and 85% on prompt signal electrons from W and Z decays.

The results on electron selection efficiencies as obtained from the "tag-and-probe" method using Z→ee events are finally presented in Table 1 and compared to Monte Carlo expectations.

	ECAL barrel			ECAL endcaps		
Selection	Efficiency data	Error (stat.+syst.)	Efficiency MC	Efficiency data	Error (stat.+syst.)	Efficiency MC
WP95%	92.5%	3.2%	95.4%	86.4%	6.7%	92.9%
WP95%	77.5%	4.7%	85.1%	75.1%	8.6%	76.2%
CiC Loose	96.4%	2.1%	97.0%	94.1%	4.7%	95.3%
CiC SuperTight	89.3%	3.4%	89.3%	85.5%	6.5%	79.4%

Table 1: Electron selection efficiency from "tag-and-probe" using Z→ee events for electron candidates in the ECAL barrel and in the ECAL endcaps and for the two cut based and category based selections.

2.2 Background studies

Several requirements are applied to tag potential background electron candidates. We first require a jet in the event with ET greater than 20 GeV and satisfying a High Level Jet Triggers. In order to eliminate tagging due to real electrons, the electromagnetic fraction of the jet is required to be less than 90%. The event must contain a reconstructed electron candidate with ET > 10 GeV which is separated from the tag jet by $\Delta R > 0.4$. The fake rate is defined as the fraction of reconstructed electron candidates that pass the background selection and a given electron ID over the total number of electron candidates passing the background selection. Figure 4 shows the fake rate as a function of ET.

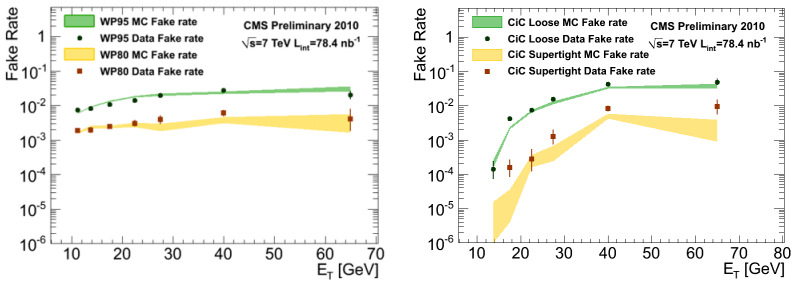

(a) (b)

Figure 4: Electron fake rate per reconstructed electron candidate as a function of ET in data and Monte Carlo for the WP95 and WP80 selections (a) and for the "CiC Loose" and "CiC SuperTight" selections (b).

3. Photon reconstruction and identification

Photons are primarily reconstructed through the energy deposited in the ECAL. The presence of material in front of the detector causes the photons to convert into electron-positron pairs. The bending of the electron and positron trajectories due to the solenoidal field leads the energy deposits to be spread along ϕ. The energy deposited in individual crystals is grouped in "superclusters". More details on photon reconstruction can be found here [7].

The energy of each photon candidate is estimated based on the ratio of the energy contained within the 3x3 array of crystals centered on the seed crystal of the photon candidate's supercluster to the total energy contained in the supercluster (r9). The r9 value is used as well to determine if the photon is converted or unconverted. To increase the purity of the photon sample additional isolation and identification requirements are applied. The photon selection is based on ECAL, HCAL and Tracker isolations and the supercluster η width. Figure 5 presents the distributions for photon candidates of some identification variables.

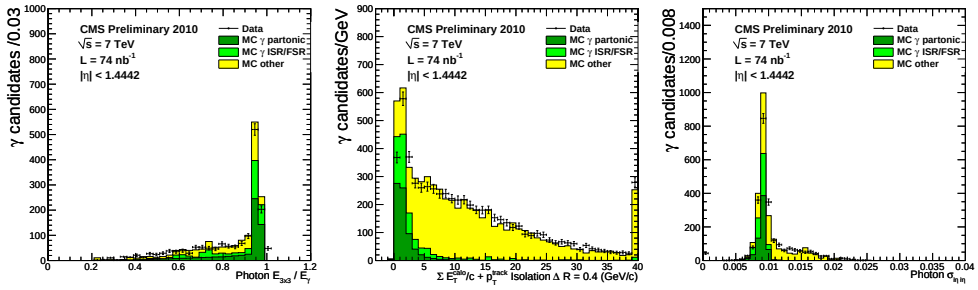

(a) (b) (c)

Figure 5: Distribution of photon identification observables: (a) the r9 variable, (b) the sum of the isolation variables (ECAL, HCAL, and Tracker) and (c) the $\sigma_{i\eta i\eta}$ shower shape. Distributions are for the ECAL barrel. The Monte Carlo results are normalized separately for each plot to the number of entries in the data histogram.

References

[1] L. Evans, (ed.) and P. Bryant, (ed.), "LHC Machine", JINST **3** (2008) S08001.

[2] R. Adolphi *et al.* [CMS Collaboration], "The CMS experiment at the CERN LHC", JINST **3** (2008) S08004.

[3] W. Adam *et al.*, "Reconstructions of Electrons with the Gaussian-Sum Filter in the CMS Tracker at the LHC", J. Phys. G: Nucl. Part. Phys. **31** (2005) N9-N20

[4] S. Baffioni *et al.*, "Electron reconstruction in CMS", Eur. Phys. J. C **49** (2007), no. 3, 1099.

[5] CMS Collaboration, Electron reconstruction and identification at at $\sqrt{s}$ = 7 TeV", CMS Physics Analysis Summary **EGM-10-004** (2010)

[6] CMS Collaboration, "Measuring Electron Efficiencies at CMS with Early Data", CMS Physics Analysis Summary **EGM-2007/001** (2008)

[7] CMS Collaboration, "Photon reconstruction and identification at $\sqrt{s}$ = 7 TeV", CMS Physics Analysis Summary **EGM-10-005** (2010)